


Why does pollen morphology vary? Evolutionary dynamics and morphospace occupation in the largest angiosperm order (Asterales)

Phillip E. Jardine^{1*} , Luis Palazzesi^{2,3*} , M. Cristina Tellería^{2,4} and Viviana D. Barreda^{2,3} 

¹Institute of Geology and Palaeontology, University of Münster, Münster 48149, Germany; ²Consejo Nacional de Investigaciones Científicas y Técnicas (CONICET), C1405DJR, Buenos Aires, Argentina; ³Sección Paleopalínología, Museo Argentino de Ciencias Naturales 'Bernardino Rivadavia', C1405DJR, Buenos Aires, Argentina; ⁴Laboratorio de Sistemática y Biología Evolutiva, Museo de La Plata, B1900FWA, La Plata, Argentina

Summary

Author for correspondence:
Phillip E. Jardine
Email: jardine@uni-muenster.de

Received: 1 December 2021
Accepted: 4 February 2022

New Phytologist (2022) **234**: 1075–1087
doi: 10.1111/nph.18024

Key words: Asterales, disparity, diversity, morphology, morphospace, phylogeny, pollen.

- Morphological diversity (disparity) is a key component of biodiversity and increasingly a focus of botanical research. Despite the wide range of morphologies represented by pollen grains, to date there are few studies focused on the controls on pollen disparity and morphospace occupation, and fewer still considering these parameters in a phylogenetic framework.
- Here, we analyse morphospace occupation, disparity and rates of morphological evolution in Asterales pollen, in a phylogenetic context. We use a dataset comprising 113 taxa from across the Asterales phylogeny, with pollen morphology described using 28 discrete characters.
- The Asterales pollen morphospace is phylogenetically structured around groups of related taxa, consistent with punctuated bursts of morphological evolution at key points in the Asterales phylogeny. There is no substantial difference in disparity among these groups of taxa, despite large differences in species richness and biogeographic range. There is also mixed evidence for whole-genome duplication as a driver of Asterales pollen morphological evolution.
- Our results highlight the importance of evolutionary history for structuring pollen morphospace. Our study is consistent with others that have shown a decoupling of biodiversity parameters, and reinforces the need to focus on disparity as a key botanical metric in its own right.

Introduction

Morphological variety, and the evolutionary processes that create and maintain it, is a fundamental component of biological diversity (Roy & Foote, 1997). Understanding how morphological diversity (termed disparity) is distributed and partitioned through time and space, and how it relates to taxonomic, phylogenetic and functional diversity (Foote, 1992; Roy & Foote, 1997; Chartier *et al.*, 2017; Mander *et al.*, 2020; Cole & Hopkins, 2021), is therefore a key goal of evolutionary (palaeo)biology, which can provide insights into questions concerning the tempo and mode of evolution, including gradual vs punctuated evolutionary models (Gould & Eldredge, 1977; Hunt, 2007; Guillerme & Cooper, 2018), extinction selectivity and postextinction recovery dynamics (Foote, 1993, 1996a; Lupia, 1999; Cole & Hopkins, 2021), and extrinsic vs intrinsic constraints on the evolution of biological form (Foote, 1994; Oyston *et al.*, 2015).

While measurement of morphological change can focus on individual traits (e.g. Hunt, 2007), greater insights are often gained by analysing suites of characters that represent biological units as a whole (Foote, 1997). In this way, morphology can be described as multivariate data (typically as discrete characters, measured continuous characters or landmarks), which are used as the basis for an ordinated morphospace and the measurement of the morphological disparity represented by a group of taxa (Foote, 1997; Hetherington *et al.*, 2015; Hopkins, 2016; Lloyd, 2016, 2018; Guillerme & Cooper, 2018; Guillerme, 2018). Phylogenetic information can be integrated directly into such analyses to provide a more detailed understanding of the drivers of morphological evolution and disparity change within a clade (Sidlauskas, 2008; Friedman, 2012; Sakamoto & Ruta, 2012; Hopkins & Smith, 2015; Cooney *et al.*, 2017; Lloyd, 2018; Woutersen *et al.*, 2018; Clark *et al.*, 2019; Mander *et al.*, 2020).

To date, the majority of morphological disparity analyses have centred on animals (e.g. Foote, 1992, 1993, 1999; Wills *et al.*, 1994; Sidlauskas, 2008; Sakamoto & Ruta,

*These authors contributed equally to this work.

2012; Hopkins & Smith, 2015; Cooney *et al.*, 2017; Cole & Hopkins, 2021), although similar approaches are increasingly being applied to both extant and fossil plant datasets. These studies have revealed that disparity tends to accumulate quickly early in the history of a clade and is typically decoupled from species richness (Lupia, 1999; Wellman *et al.*, 2013; Oyston *et al.*, 2016; Mander, 2018; Chartier *et al.*, 2021) and that morphological variability is related to both phylogeny (Chartier *et al.*, 2017; Kriebel *et al.*, 2017; Clark & Donoghue, 2018; Woutersen *et al.*, 2018; Clark *et al.*, 2019; Mander *et al.*, 2020; Bogotá-Ángel *et al.*, 2021) and functional ecology (Chartier *et al.*, 2017; Kriebel *et al.*, 2017; Mander *et al.*, 2020), similar to the trends recorded previously in animal groups (e.g. Foote, 1993, 1994; Friedman, 2012; Hughes *et al.*, 2013; Hopkins & Smith, 2015). While whole-genome duplication (WGD) has previously been linked to plant diversification and morphological innovation (Soltis & Soltis, 2016; Landis *et al.*, 2018), there is mixed evidence for WGD as a driver of variations in disparity or morphospace occupation among clades: although Clark & Donoghue (2018) demonstrated a link between WGD and morphological innovation in angiosperms, Clark *et al.* (2019) found that this was not supported in horsetails.

Pollen grains and spores (collectively sporomorphs) have evolved into a wide variety of shapes and sizes, with a range of external ornamentation, wall structures and aperture styles (Traverse, 2007; Mander, 2016). As the reproductive vectors of plants, sporomorphs play a vital role in the transfer of genetic material and the maintenance of plant populations (Traverse, 2007). The outer wall (exine) of sporomorphs also has an excellent preservation potential in the geological record due to its constituent biopolymer sporopollenin (Ariizumi & Toriyama, 2011; Fraser *et al.*, 2012; Mackenzie *et al.*, 2015), making the fossil sporomorph record one of the key indicators of plant macroevolution, palaeoecology and palaeobiogeography (e.g. Jaramillo *et al.*, 2006; Wellman *et al.*, 2013). Yet, there is considerable uncertainty regarding the evolutionary processes that have generated the morphological diversity found across the sporomorphs of extant plants, and in particular, the wide range of morphologies displayed by angiosperm (flowering plant) pollen (Mander, 2016). In particular, there are substantial knowledge gaps concerning the links between pollen morphological evolution and phylogeny, environment (including water stress and volumetric responses to dehydration), function (including pollination ecology), animal pollinator evolution and possible correlations with morphological evolutionary dynamics of other plant organs (Traverse, 2007; Kriebel *et al.*, 2017; Mander *et al.*, 2020). Knight *et al.* (2010) demonstrated that genome size is a poor predictor of pollen size, but to our knowledge, there have been no analyses of how genome size or WGD events relate to pollen morphological evolution and disparity.

Here, we address these uncertainties by analysing Asterales pollen morphological evolution in a phylogenetic context, generating a pollen phylomorphospace and measuring morphological disparity and rates of morphological evolution through time and

across the Asterales phylogeny. Asterales, which includes the daisy family (Asteraceae or Compositae) and bell flowers (Campanulaceae), is one of most diverse angiosperm orders, with a cosmopolitan biogeographic distribution that encompasses all continents except Antarctica (Mandel *et al.*, 2019; McDonald-Spicer *et al.*, 2019). The evolutionary history of the Asterales extends back to the Cretaceous, with a Gondwanan origin and subsequent spread across the globe, and an explosive radiation of lineages during the late Eocene to Miocene (Barreda *et al.*, 2010a, 2015; Mandel *et al.*, 2019; Palazzesi *et al.*, 2022). The majority of the taxonomic diversity in Asterales is concentrated in Asteraceae, and in Asteraceae within the subfamilies Asteroideae (which includes daisies and sunflowers), Cichorioideae (which includes lettuce and dandelions) and Carduoideae (thistles) (Panero & Crozier, 2016; Mandel *et al.*, 2019) (Fig. 1). Asterales incorporates a wide variety of pollen morphologies, including variations in size, shape, wall structure and ornamentation (Wortley *et al.*, 2007, 2008, 2012; Blackmore *et al.*, 2009, 2010; Katinas *et al.*, 2010; Barreda *et al.*, 2015; Inchaussandague *et al.*, 2018) (Fig. 2), making them an ideal group for understanding the drivers and constraints on pollen morphological evolution, and through this obtaining insights into the generation and maintenance of botanical diversity. While there have already been many years of research into Asteraceae pollen morphology, and more recently its evolution in the context of molecular phylogenies (Wortley *et al.*, 2008; Blackmore *et al.*, 2009; Barreda *et al.*, 2015), this has not yet been considered in the framework of morphospace occupation, disparity and evolutionary rates, or across the Asterales as a whole.

Materials and Methods

Phylogenetic tree assembly

We used a backbone tree of Asterales derived from a calibrated molecular analysis from Barreda *et al.* (2015) with 33 tips and included 80 additional taxa of the family Asteraceae from a more recent calibrated phylogenetic tree from Mandel *et al.* (2019). Both chronograms were grafted using the function 'paste.tree' from the R package PHYTOOLS (Revell, 2012). We pruned the phylogenetic tree and kept 113 taxa that represent most of the tribes within the order Asterales from which we could retrieve pollen characters.

Morphological character coding

Pollen characters for 113 extant species were obtained either from the examination of slides of acetolysed pollen grains housed at herbaria (ALCB, B, BAF, C, CANB, CBG, FM, G, GÖTT, HAC, HAJB, HUT, K, LP, MO, S, US and WIS; Index Herbariorum <http://sweetgum.nybg.org/science/ih/>) or from the literature (Jiménez *et al.*, 2004; Tellería & Katinas, 2004, 2009; Tellería, 2008, 2017; Tellería *et al.*, 2010, 2013; Barreda *et al.*, 2015). The morphological matrix comprises 28 binary and multistate discrete characters, details of which are provided in Supporting Information Table S1.

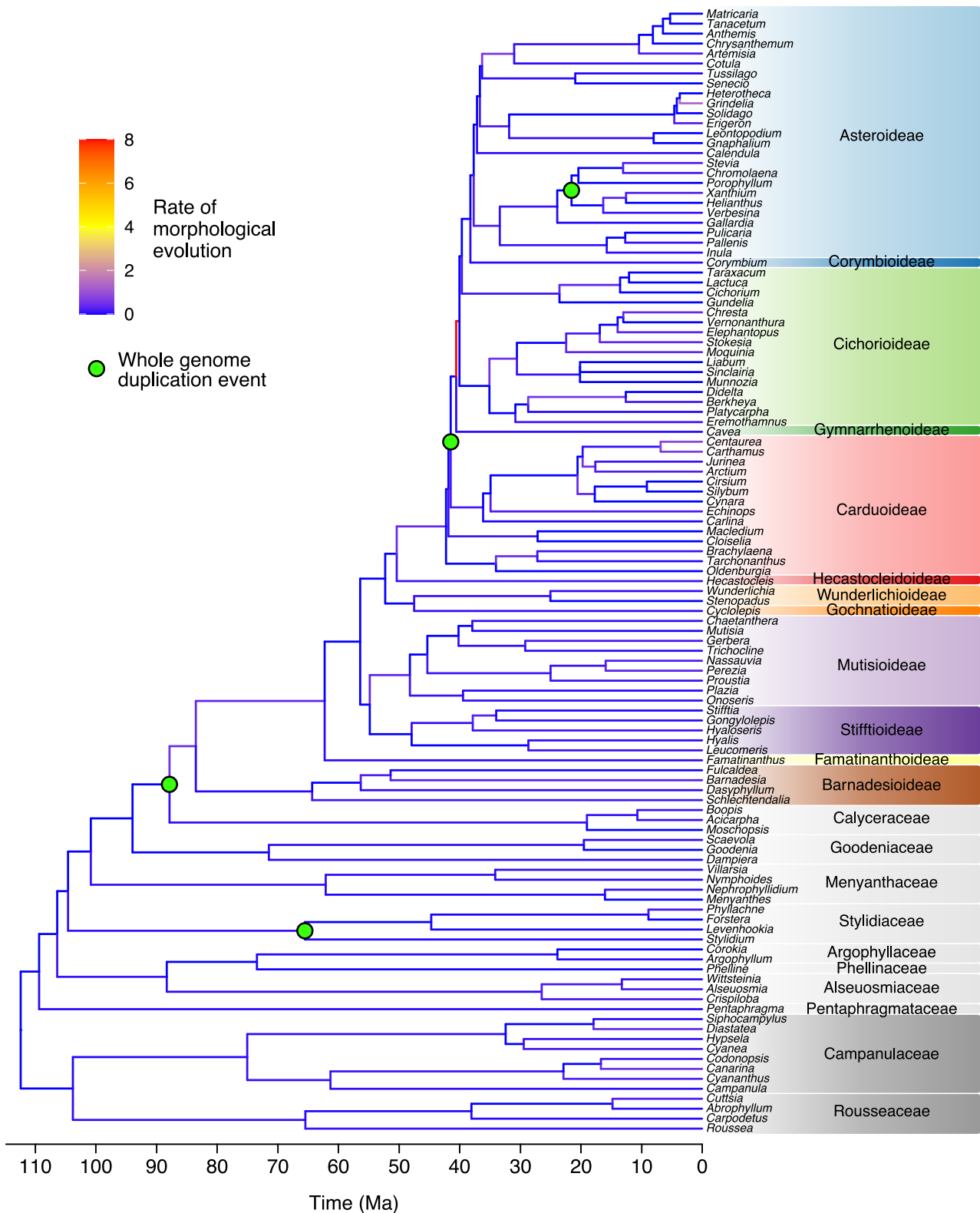


Fig. 1 Molecular phylogeny of the Asterales taxa in this study. Branches are coloured by rates of morphological evolution. Whole-genome duplication (WGD) events are from Barker *et al.* (2008, 2016) and Landis *et al.* (2018). Ma, million years ago.

Phylomorphospace and disparity analysis

We produced a phylomorphospace (i.e. with the taxa and phylogeny plotted in the same morphospace) (Sidlauskas, 2008;

Sakamoto & Ruta, 2012; Hopkins & Smith, 2015; Hopkins, 2016; Lloyd, 2016, 2018; Clark & Donoghue, 2018; Woutersen *et al.*, 2018) following the workflow outlined in Lloyd (2016, 2018). First, we reconstructed the ancestral

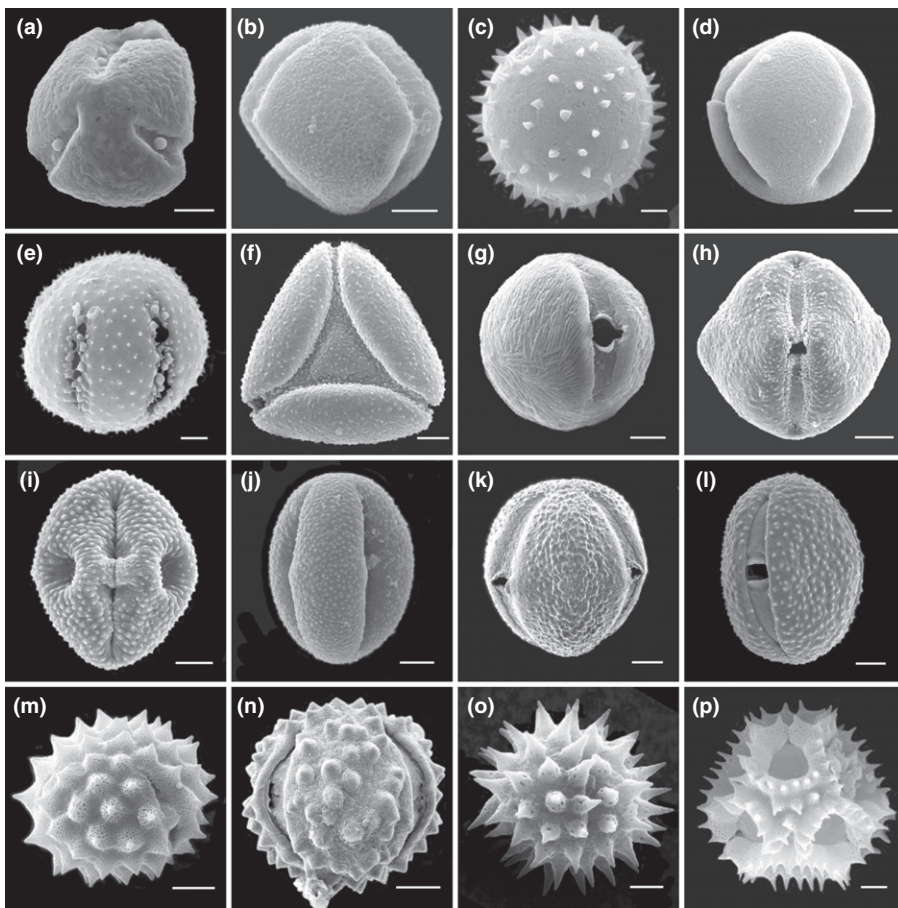


Fig. 2 Scanning electron microscopy (SEM) images of selected asteralean pollen grains (a) *Alseuosmia macrophylla* (Alseuosmiaceae); (b) *Corokia cotoneaster* (Argophyllaceae); (c) *Campanula barbata* (Campanulaceae); (d) *Cuttsia viburnea* (Rousseaceae); (e) *Stylidium albililaceum* (Stylidiaceae); (f) *Nymphoides indica* (Menyanthaceae); (g) *Anthotium humile* (Goodeniaceae); (h) *Boopis anthemoides* (Calyceraceae); (i) *Schlechtendalia luzulaefolia* (Asteraceae Barnadesioideae); (j) *Chuquiraga erinacea* (Asteraceae Barnadesioideae); (k) *Gochnatia spectabilis* (Asteraceae Gochnatioideae); (l) *Mutisia pulcherrima* (Asteraceae, Mutisioideae); (m) *Carduus thoermeri* (Asteraceae Carduoideae); (n) *Wunderlichia cruelsiana* (Asteraceae Wunderlichioideae); (o) *Porophyllum ruderale* (Asteraceae Tageteae); and (p) *Picris echioides* (Asteraceae Cichorieae). Scale bars: 5 μ m (b–k, p); 10 μ m (a, l, m, n); 2 μ m (o).

character states for the nodes of the phylogeny using maximum likelihood estimation (Lloyd, 2018) and then ordinated both the tips and the nodes of the phylogeny using principal coordinates analysis (PCO) of an arcsine square root transformed Maximum Observable Rescaled Distance (MORD) distance matrix (Lloyd, 2016, 2018). This corresponds to the ‘pre-ordination ancestral state estimation’ (pre-OASE) approach of Lloyd (2018). Eleven of the 28 characters (principally those that related to size and shape; see Table S1) were treated as ordered in the analysis, although preliminary data exploration suggested that treating all characters as unordered did not substantially alter the result. Seven characters were treated as secondary characters *sensu* Hopkins & St John (2018); that is, whether they are coded as applicable or inapplicable for each taxon will depend on the state of their associated primary character (characters relating to colpi morphology depend on the taxon being coded as colpate rather than porate, for example, and for porate taxa, the colpi morphology character would be treated as inapplicable; see Table S1). The primary characters were scaled by setting the parameter α to 0.5 (see Hopkins & St John (2018) for further information). The PCO was carried out with Cailliez correction to ensure that only non-negative eigenvalues were produced (Cailliez, 1983). We also produced a chronophylomorphospace (Sakamoto & Ruta, 2012) by plotting the first two PCO axis scores against a third time axis, using the estimated tip and node ages to plot the taxa and the phylogeny.

We estimated the phylogenetic signal of the tip scores on each ordination axis using Blomberg’s K (Blomberg *et al.*, 2003), with statistical significance assessed via a permutation test with 1000 randomizations. Blomberg’s K equals 1 under a Brownian motion model of trait evolution, with values higher than 1 indicating that closely related tips are more similar to each other than expected under Brownian motion (high phylogenetic signal), and values lower than 1 indicating that closely related tips are less similar than expected under Brownian motion (low phylogenetic signal).

Principal coordinates analysis applied to discrete character data often suffers from the variance in the data being diffused over many axes, rather than being concentrated on the first few (Lloyd, 2016). This means a (phylo)morphospace constructed from the first two PCO axes may only account for a small percentage of the variance in the data (Lloyd, 2016). We therefore explored other multivariate techniques for visualizing these data, specifically a phylomorphospace constructed from a two-axis nonmetric multidimensional scaling (NMDS) ordination solution, cluster analysis and a Neighbor-Net phylogenetic network (Bryant & Moulton, 2004). All were applied to an arcsine square root transformed MORD distance matrix as described earlier, with the NMDS ordinating both the tips and the reconstructed ancestral states for the nodes (as with the PCO, above), and the cluster analysis and Neighbor-Net applied to just the intertaxon pairwise distances (i.e. just the tips of the phylogeny). Finally, we

followed previous authors (Hopkins & Smith, 2015; Woutersen *et al.*, 2018) in carrying out a PCO of the intertaxon distances, and using the PCO axis scores as new continuous characters to reconstruct ancestral states for the nodes of the phylogeny, before adding these to the ordination to produce a phylomorphospace (this corresponds to the ‘postordination ancestral state estimation’ or post-OASE approach of Lloyd (2018)).

We tabulated morphological disparity both within clades and through time. For the within-clades analysis, the genera were divided into four groups: ‘Campanulaceae/Rousseaceae’, which is the sister clade to the rest of the Asterales; ‘Core Asterales’, comprising the Asterales families excluding Campanulaceae, Rousseaceae and Asteraceae; ‘Asteraceae 1’, comprising the subfamilies that diverged before transcontinental dispersal of Asteraceae out of South America (Panero & Crozier, 2016), which include Barnadesioideae, Famatinanthoideae, Stifftioideae, Mutisioideae, Gochnatioideae, Wunderlichioideae and Hecastocleidoideae; and ‘Asteraceae 2’, comprising the subfamilies that diverged after this transcontinental dispersal out of South America, which include Carduoideae, Gymnarrhenoideae, Cichorioideae, Corymbioideae and Asteroideae (Fig. 1). The Asteraceae 2 group is synonymous with the African Asteraceae Dispersion or AAD clade of Panero & Crozier (2016) and corresponds to the Asteraceae clade that underwent an explosive diversification and near-global dispersal *c.* 40 Ma (Panero & Crozier, 2016; Mandel *et al.*, 2019). Disparity within each clade was measured as the sums of variances of the PCO axis scores and the median distance to the multivariate centroid, and as an ordination-free comparison as the mean pairwise MORD distance (Lloyd, 2016). In each case, just the tips of the phylogeny were included in the calculation, with 1000 bootstrapped replicates to generate a distribution of values (Guillerme, 2018). To check the influence of group membership on the results, disparity was also measured with Carduoideae included in the Asteraceae 1 clade, and with the Campanulaceae/Rousseaceae and Core Asterales groups combined into one ‘Ancestral Asterales’ group.

We calculated disparity through time using the time slicing method of Guillerme & Cooper (2018). This approach uses a time-calibrated phylogeny to estimate lineage presence through time, which allows disparity to be measured at equidistant time slices. As with the within-clades analysis, we used the sums of variances of the ordination axis scores, the median distance to the multivariate centroid and the mean pairwise MORD distance as measures of disparity. These were calculated at 5-million-year intervals, with the median, 2.5% and 97.5% percentiles of 1000 bootstrapped replicates giving the disparity estimate and associated confidence intervals. When branches of a phylogeny are used for calculating disparity, it is necessary to select either the ancestral node or the descendent node/tip, which are chosen according to a predetermined model of character evolution (Guillerme & Cooper, 2018). We assumed a gradual evolutionary model, using the ‘gradual splits’ model of Guillerme & Cooper (2018), which selects either the ancestor or descendent for each bootstrap replicate with a probability calculated as the distance between the ancestor and the time slice as a proportion of the total branch length. For comparison, we also calculated disparity through time

using the ‘acctran’ (accelerated transformation, which always uses the descendent) and ‘deltran’ (delayed transformation, which always uses the ancestor) models of Guillerme & Cooper (2018).

Evolutionary rate measurements

Evolutionary rates were measured as the mean number of character state changes per million years, following the procedure of Lloyd (2016). Rates were measured for each branch of the phylogeny, and through time via the sum of character state changes across the phylogeny within 22 evenly spaced time bins. For the branch rates, statistically significant high or low values on each branch relative to the rest of the tree were identified following Lloyd *et al.* (2012). For each branch in turn, this approach uses a likelihood ratio test to assess whether a one-rate model (with one overall rate for the whole tree) or a two-rate model (with one rate for the branch in question and one rate for the rest of the branches pooled together) is preferred, with the Benjamini–Hochberg correction (Benjamini & Hochberg, 1995) applied to the *P* value to account for multiple comparisons and an alpha value of 0.01 used to determine a statistically significant result (Lloyd *et al.*, 2012; Lloyd, 2016). For the rates through time, the timing of the character state changes on each branch was drawn at random from a uniform distribution, and the calculation repeated 1000 times (Lloyd *et al.*, 2012; Lloyd, 2016). The time bin medians and 2.5% and 97.5% percentiles were then extracted to produce an estimate of evolutionary rates with a 95% confidence interval.

Phylogenetic diversity and lineages through time

Phylogenetic diversity was measured for each of the four clades (see earlier) to provide an estimate of the amount of evolutionary history encompassed by each clade (Chao *et al.*, 2010). We measured phylogenetic diversity using Faith’s phylogenetic diversity (PD), which is calculated as the sum of the branch lengths connecting the tips (taxa) within each clade (Faith, 1992), and is a phylogenetic generalization of species richness (Chao *et al.*, 2010, 2014). We also tabulated lineages through time (LTT) to give an estimate of temporal patterns in species richness represented by the phylogeny.

Biogeography and whole-genome duplication data compilation

We compiled the biogeographic distribution of the taxa used in this study from Kadereit & Jeffrey (2007). The position of WGD events on the Asterales phylogeny was taken from Barker *et al.* (2008, 2016) and Landis *et al.* (2018).

Software and reproducibility

Data analysis was carried out in R v.4.0.4 (R Core Team, 2021) with RSTUDIO v.1.4.1717 (R Studio Team, 2021), using the packages APE v.5.4-1 (Paradis & Schliep, 2019), CLADDIS v.0.6.3 (Lloyd, 2016), DISPARITY v.1.5.0 (Guillerme, 2018), DPLYR v.1.0.7

(Wickham *et al.*, 2021), GGTREE v.3.0.4 (Yu *et al.*, 2017), PHANGORN v.2.8.0 (Schliep, 2011), PHYTOOLS v.0.7-70 (Revell, 2012), PICANTE v.1.8.2 (Kembel *et al.*, 2010), PLOT3D v.1.3 (Soetaert, 2019), RCOLORBREWER v.1.1-2 (Neuwirth, 2014), SCATTERPIE v.0.1.7 (Yu, 2020), VEGAN v.2.5-7 (Oksanen *et al.*, 2020) and VELOCIRAPTR v.1.1.0 (Zaffos, 2019). The Neighbor-Net phylogenetic network was produced using SPLITS TREE4 v.4.17.1 (Huson & Bryant, 2006), using a MORD distance matrix exported from R. All data files and R code used in this analysis are available for download from figshare (Jardine *et al.*, 2022).

Results

Arrangement of taxa in morphospace

The arrangement of taxa on the first two principal coordinates of the phylomorphospace shows three main clusters, arranged according to the Asterales phylogeny (Figs 1, 3). The lower left cluster incorporates the ancestral Asterales (i.e. the Asterales

excluding Asteraceae), including the monophyletic Campanulaceae/Rousseaceae clade and the paraphyletic group of other non-Asteraceae families ('Core Asterales') (Fig. 3). The lower right cluster comprises Asteraceae 1 clade, with Barnadesioideae transitional between these taxa and the ancestral Asterales. The third cluster, which occurs at higher values on PCO 2, comprises the Asteraceae 2 clade with subfamilies Asteroideae, Corymbioideae, Cichorioideae and Gymnarrhenoideae, with Carduoideae as morphologically transitional between the Asteraceae 1 and 2 groups (Fig. 3). Exceptions to this general pattern are *Barnadesia* (Barnadesioideae), which is placed with the Asteraceae 2 cluster, and the Asteroideae tribe Anthemideae, which occurs closer to the Asteraceae 1 cluster. The first two principal coordinates contain a strong and statistically significant phylogenetic signal (for PCO 1 $K=2.31$, $P=0.001$, and for PCO 2 $K=1.24$, $P=0.001$; $n=113$ in each case; see also Fig. S1).

Low variance accounting on the highest principal coordinates is a common problem with discrete character morphospace analysis (Lloyd, 2016). Here, the first two principal coordinates account for <10% of the variance in the dataset, with the remaining variance spread over 221 principal coordinates. The higher axes are less easy to explain in terms of within- and among-clade relationships (Fig. S2a,b), and there is a lower phylogenetic signal beyond the first two axes (for most axes $K<0.5$; Fig. S1). Alternative multivariate methods such as NMDS (Fig. S2c), cluster analysis (Fig. S3) and Neighbor-Net (Fig. S4), as well as a post-OASE PCO (Fig. S2d), reveal a similar pattern to that shown on the first axes of the pre-OASE PCO (Fig. 3). Therefore, the two-axis phylomorphospace presented here (Fig. 3) captures the main signal in the data, despite the high proportion of variance distributed over the remaining principal coordinates.

The first principal coordinate is explained by variations in pollen size and shape, with smaller, more oblate (equatorial axis > polar axis) grains on the left of the morphospace (negative PCO values, the ancestral Asterales cluster and the Asteraceae 2 cluster), and larger, more prolate (equatorial axis < polar axis) grains on the right (positive PCO values, comprising the Asteraceae 1 cluster) (Figs 2, S5). There is also a gradient of pollen wall complexity on the first principal coordinate, with thinner, simpler walled taxa having more negative PCO values, and thicker, more complex walled taxa (i.e. with an internal tectum, more ectexinal layers and more clearly distinguishable columellae) having more positive PCO values (Fig. S5). The second principal coordinate is primarily related to sculpture, with genera at the upper end of the axis (the Asteraceae 2) being echinate and genera at the lower end of the axis representing a range of sculptural types. Specifically, the Asteraceae 1 are dominated by microechinate grains, and the ancestral Asterales comprise a range of different sculptural forms including rugulate, striate, verrucate and microechinate grains (the Campanulaceae/Rousseaceae clade is more sculpturally variable, while the other non-Asteraceae families are predominantly microechinate) (Figs 2, S5).

This distribution of character scores across morphospace explains why some taxa occur outside of the main clusters occupied by their close relatives. For example, Anthemideae occurs

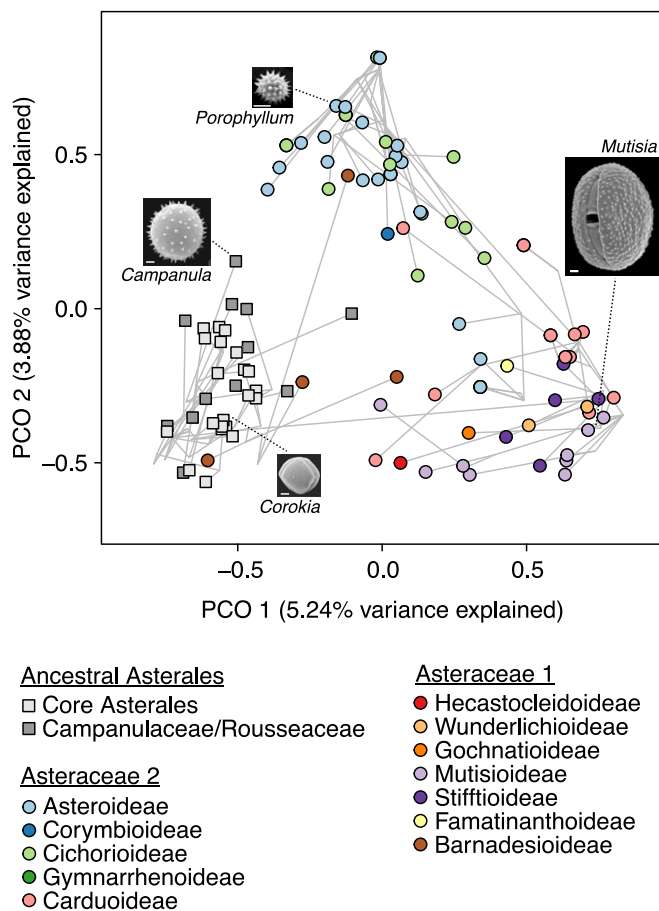


Fig. 3 Phylomorphospace constructed from the first two axes of a principal coordinates analysis (PCO). Point colours match the family/subfamily colours in Fig. 1. Values in parentheses are the percentage variance explained by each PCO axis. Scanning electron microscopy (SEM) images show taxa that are representative for the different regions of morphospace; scale bars equal 5 μm (note that for clarity *Porophyllum* is shown at twice the size relative to the other taxa).

closer to the Asteraceae 1 cluster because these taxa possess thicker exines with a more complex internal structure, and in the case of *Artemisia* (mugwort or sagebrush), smaller echinae. Similarly, *Barnadesia* is both cavate and lophate, in common with taxa in Cichorioideae such as *Lactuca* (lettuce) and *Taraxacum* (dandelions), and as such occurs closer to the Asteraceae 2 cluster.

Morphological disparity

Morphological disparity is lowest in the Campanulaceae/Rousseaceae clade, and similar in the core Asterales, the Asteraceae 1 and the Asteraceae 2 (Figs 4a, S6a), although measuring disparity as the mean pairwise MORD distance (i.e. using the distance matrix directly, rather than working with the axis scores of the ordination) leads to a lower disparity in the Asteraceae 2 clade (Fig. S6b). A similar pattern is demonstrated if Carduoideae are combined with the Asteraceae 1 (Fig. S6c), and if the Campanulaceae/Rousseaceae clade is combined with the other non-Asteraceae Asterales to form an ancestral Asterales group, with all three groups incorporating a similar disparity (Fig. S6d). Phylogenetic diversity (measured as Faith's PD) is also lowest in the Campanulaceae/Rousseaceae relative to the other three clades, with the Asteraceae 2 having the highest PD (Fig. 4b). There is no relationship between within-clade disparity and species richness (Fig. 4).

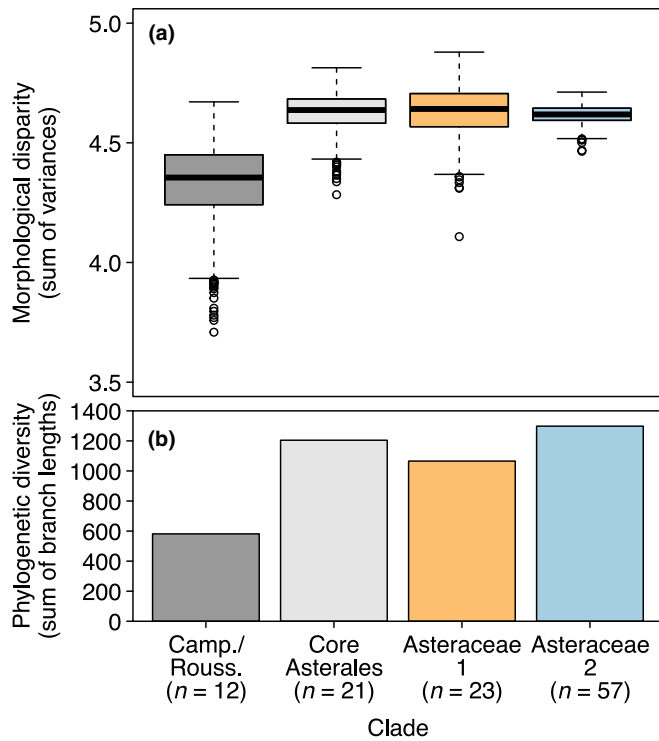


Fig. 4 Within-group morphological disparity (a) and phylogenetic diversity (b). Morphological disparity in (a) was calculated via the sums of variances of the ordination axes, and the boxplot shows the distribution of values from 1000 bootstrapped replicates. For the boxplots, the thick horizontal bars show the median, the edges of the boxes show the lower and upper quartiles, error bars (whiskers) show the extent of values up to 1.5 times the interquartile range, and the circles show the outliers beyond this limit.

Asterales morphological disparity through time shows a rapid increase at the start of the timeseries, followed by a gradual increase from *c.* 100 Ma to *c.* 50 Ma, at which point the curve begins to level off and disparity accumulates more slowly through to the present (Fig. 5a). This pattern is robust to using other evolutionary models (acctran and deltran) or measuring disparity as the median distance to centroid rather than sums of variances, although the mean pairwise MORD distance suggests a more gradual accumulation of disparity in the first part of the timeseries (Fig. S7). Adding a temporal axis to the 2-dimensional morphospace in Fig. 3 to produce a chronophylomorphospace shows the large increase in morphospace occupation in the first half of the timeseries with the appearance of the Asteraceae 1 cluster (Fig. 6), which coincides with the accumulation of disparity early

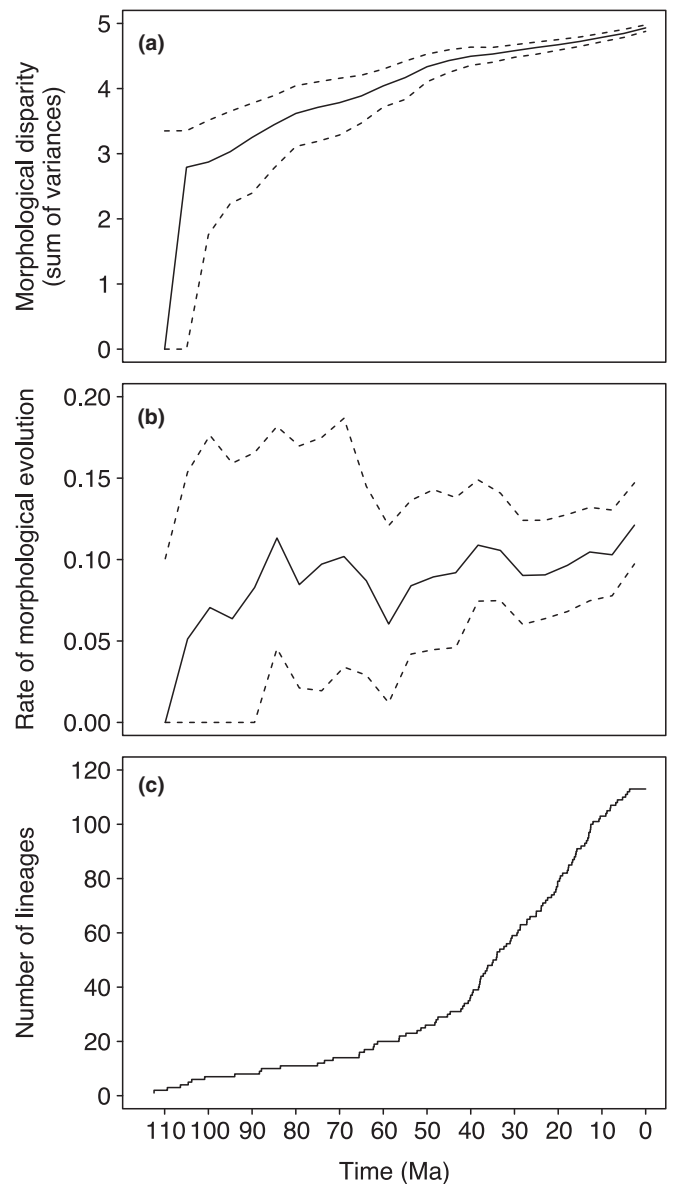


Fig. 5 Morphological disparity (a), rates of morphological evolution (b) and number of lineages (c) through time. Dashed lines in (a, b) are 95% confidence intervals. Ma, million years ago.

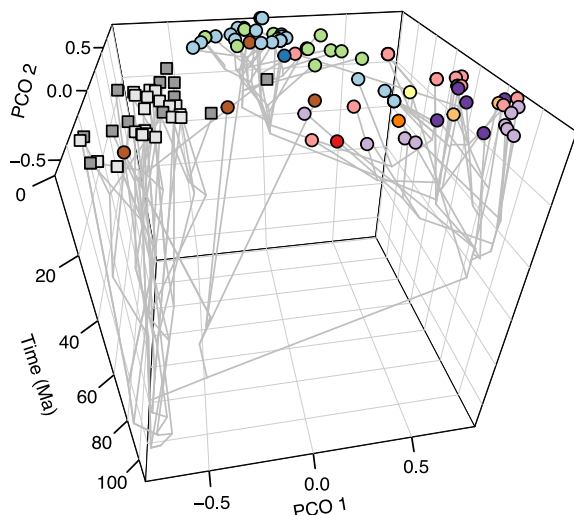
in the Asterales evolutionary history (Fig. 5a). The subsequent appearance of the Asteraceae 2 cluster as another punctuated shift in morphospace occupation *c.* 40–50 Ma shows that this group diversified in a relatively restricted area of morphospace (Figs 3, 6) and without a substantial contribution to total disparity (Fig. 5a).

Rates of morphological evolution

Rates of morphological character change increase sharply at the beginning of the timeseries, and then are broadly stable through to the present, aside from a possible slight decrease *c.* 60 Ma and a slight increase from *c.* 20 Ma onwards; the 95% confidence interval is also wider between *c.* 110 and 60 Ma, indicating greater uncertainty in the reconstruction and the potential for higher or lower rates though the Late Cretaceous relative to the Cenozoic (Fig. 5b). Morphological rates are broadly stable across the Asterales phylogeny, with no clades or lineages showing markedly higher rates than others (Fig. 1). Only two branches show statistically significantly higher rates of morphological evolution compared to the rest of the phylogeny. One is the branch leading to the Cichorioideae, Corymbioideae and Asteroideae clades, which correspond to a pronounced shift in morphospace occupation (Figs 3, 6) and the highest branch rates across the phylogeny (8.00 character state changes/Ma, $P = 1.80 \times 10^{-7}$, Benjamini–Hochberg corrected $\alpha = 4.46 \times 10^{-5}$) (Fig. 1). The other is the terminal branch leading to *Grindelia* (Asteroideae and Astereae) (1.41 character state changes/Ma, $P = 3.22 \times 10^{-5}$, Benjamini–Hochberg corrected $\alpha = 8.93 \times 10^{-5}$), which differs from the rest of the Astereae taxa in possessing rounded rather than acute colpi ends, scabrate rather than psilate apertural membranes, a psilate rather than scabrate or microperforate tectal surface among the major sculptural elements, a relatively thinner exine at the grain equator and a lower nexine : sexine (inner : outer exine) ratio.

Morphological evolution and whole-genome duplication events

Reconstructed WGD events are located at the split between Calyceraceae and Asteraceae *c.* 90 Ma, at the base of the



Stylidiaceae *c.* 65 Ma, at the split between the Carduoideae tribe Cynareae (the thistles) and the Gymnarrhenoideae/Cichorioideae/Corymbioideae/Asteroideae clade *c.* 40 Ma, and within the Asteroideae supertribe Helianthodae *c.* 20 Ma (Fig. 1). The WGD events at the Asteraceae/Calyceraceae split and within the Carduoideae occur at or close to shifts in morphospace occupation and the appearance of the Asteraceae 1 and Asteraceae 2 groups, respectively (Figs 3, 6), with an associated increase in lineage richness in the case of the Carduoideae WGD event (Fig. 5c). However, the WGD events at the base of the Stylidiaceae and within the Helianthodae do not appear to be linked to any obvious changes in morphospace occupancy or evolutionary rates (Figs 1, 3), and there is no obvious relationship between within-clade morphological disparity and the location of WGD events on the Asterales phylogeny (Fig. 4).

Morphological evolution and biogeography

The ancestral Asterales taxa (Fig. 3) occur predominantly in Oceania, although Campanulaceae has a cosmopolitan distribution, and Calyceraceae is limited to South America (Fig. S8). The Asteraceae 1 taxa are mostly limited to South America, while the Asteraceae 2 are much more widely spread, including some individual taxa with cosmopolitan distributions (Fig. S8). Carduoideae occur as an intermediate group, with some taxa (e.g. *Brachylaena*, *Cloiselia* and *Oldenburgia*) being limited to Africa, while others (members of the thistle tribe Cynareae such as *Carthamus* and *Cirsium*) have a wider distribution (Fig. S8). These biogeographic results are in good agreement with previous analyses of ancestral ranges and dispersal routes, with a Gondwanan origin of the Asterales, and the spread to Africa and subsequent diversification and dispersal of the derived subfamilies *c.* 40 Ma (Panero & Crozier, 2016; Mandel *et al.*, 2019) (Fig. 6).

Discussion

Variations in morphospace occupation can manifest themselves either as differences in the *region* of morphospace occupied by groups of taxa, the *amount* of morphospace occupied

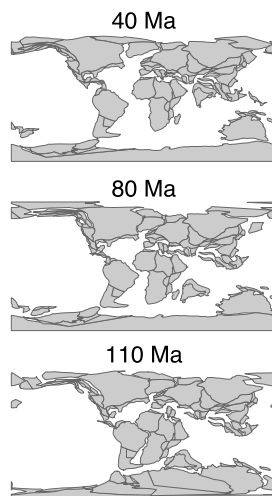


Fig. 6 Chronophylomorphospace, showing the phylomorphospace from Fig. 3 with a third time axis, and palaeogeographic maps showing the positions of the continents at key points in Asterales evolutionary history (the first appearance of the Asterales *c.* 110 million years ago (Ma), the first appearance of Asteraceae *c.* 80 Ma and the first appearance of the Asteraceae 2 clade *c.* 40 Ma). Point colours and styles in the chronophylomorphospace are the same as for Fig. 3, with grey squares denoting the non-Asteraceae Asterales, and the coloured circles denoting Asteraceae taxa (coloured by subfamily). PCO, principal coordinates analysis

(i.e. disparity), or both (these parameters are also referred to as location vs scale effects, see Warton *et al.* (2012) for details). Our results from Asterales pollen demonstrate considerable evidence for the former, with a partitioning of morphological space into distinct groupings of taxa based on major clades, leading to a phylogenetically structured pattern of morphospace occupation (Fig. 3). There is limited support for differences in disparity among the clades examined here, aside from a slightly lower disparity in the Campanulaceae/Rousseaceae clade, despite substantial variations in species richness, phylogenetic diversity and biogeographic range (Figs 4, S8). Similarly, there are no clear clade-based variations in rates of morphological evolution across the Asterales phylogeny (Fig. 1).

The temporal pattern of disparity reconstructed here, with a more rapid early increase followed by saturation, is consistent with previous analyses of both extant and fossil organisms (Foote, 1994; Lupia, 1999; Oyston *et al.*, 2015, 2016; Cooney *et al.*, 2017), as is the discordance between morphological disparity and taxonomic richness (Foote, 1993, 1996b; Lupia, 1999; Oyston *et al.*, 2016) (Fig. 5). While the early increase in disparity and evolutionary rates can in part be attributed to the appearance of Asteraceae *c.* 85 Ma, the diversification of the subfamilies in the Asteraceae 2 clade *c.* 40 Ma does not drive a further substantial disparity increase (Figs 1, 5a, S7). Despite the lack of sustained increase in disparity and the apparent saturation of morphological space, there is no reduction in the rate of morphological evolution, which has remained more or less stable through the Cenozoic (Fig. 5b). These results suggest that the derived Asteraceae pollen types evolved in already occupied morphological space (Cooney *et al.*, 2017), using a recombination of existing morphological traits (e.g. smaller pollen with a simpler wall structure that also occurs in the ancestral Asterales) as well as the development of longer, more sparsely distributed spines (echinae) on the pollen surface, and in the case of some members of the Cichorioideae ridges (lophae) across the grain (Fig. 2).

A key question is whether the punctuated bursts of evolution in pollen form identified here represent a genuine signal, and therefore support a punctuated rather than gradual model of morphological evolution, or are the result of extinction removing intermediate morphologies (Gould & Eldredge, 1977; Deline *et al.*, 2018; Sauquet & Magallon, 2018). This question can only be answered with the inclusion of fossil data, however, which is beyond the scope of this study (see later for further discussion). However, whether these shifts in morphospace occurred rapidly or over longer time periods, they still represent macroevolutionary change, which demands an explanation for why they occur at certain points in the Asterales phylogeny. One potential causal mechanism is WGD events, which have been correlated with floral morphological evolution and taxonomic diversification in a range of plant groups (Soltis *et al.*, 2009; Soltis & Soltis, 2016; Clark & Donoghue, 2018; Landis *et al.*, 2018). Furthermore, several WGD events have been identified within the Asterales (Fig. 1) (Barker *et al.*, 2008, 2016; Landis *et al.*, 2018). The relationship between WGD events and the morphological developments reconstructed here is complicated, however. On one hand, WGD events coincide with the formation of major groups in

morphospace: WGD at the split between Asteraceae and Calyceraceae may have contributed to the appearance of the Asteraceae 1 cluster in the phylomorphospace, and proposed WGD within the Cardioideae may have triggered or enabled the evolution of smaller, echinate pollen grains with a simpler internal wall structure (and lophae in the Cichorioideae) within Asteraceae 2 (Figs 3, 6). On the other hand, the WGD event at the Asteraceae/Calyceraceae split did not drive changes in Calyceraceae pollen morphology, and there was no obvious morphological response following WGD events at the base of the Stylidiaceae or nested within the Helianthodae supertribe of the Asteroideae. Furthermore, the most pronounced morphological development within the Asteroideae occurs at the base of the Anthemideae tribe, which occurs closer to the Asteraceae 1 cluster in the phylomorphospace (Fig. 3), yet this change in pollen form does not coincide with a WGD event (Fig. 1).

A particular challenge with predicting the likely response to WGD events is understanding the genetic controls on pollen morphological development and how genome duplication can impact on this (Nadot *et al.*, 2008; Soltis *et al.*, 2009; Blackmore *et al.*, 2010; Matamoro-Vidal *et al.*, 2016). It may be that WGD events provide the potential for morphological evolution in pollen, but do not have a predictable response or rely on interactions with other variables, such as evolution in other morphological or functional traits within the parent plants. Despite these complications, the occurrence of WGD events close to large-scale shifts in morphospace occupation is interesting and suggestive enough to warrant further investigation, especially since at least one of these coincides with a large increase in diversification and dispersal within the Asteraceae (Panero & Crozier, 2016; Mandel *et al.*, 2019). More targeted analyses may therefore be able to uncover whether there is a causal link between WGD and pollen morphological evolution, and how it operates to drive evolution in pollen form in some cases but not others.

In contrast to the findings of Clark & Donoghue (2018) on an angiosperm-wide dataset, our results do not support a difference in disparity among either the higher taxa analysed here (Fig. 4), or the individual Asteraceae subfamilies (Fig. S9), and there are no obvious changes in morphological variability following WGD events. This is particularly remarkable in the derived Asteraceae, and especially Asteroideae, which has a high diversity (comprising > 70% of Asteraceae species; Panero & Crozier, 2016) and a cosmopolitan distribution (Mandel *et al.*, 2019) (Fig. S8), while maintaining a relatively conserved pollen morphology with limited evidence for continued morphological innovation (Figs 2o, 3). However, it is also the case that conserved pollen morphologies within plant taxa (typically genera or higher) are common, which leads to the persistent problem of low taxonomic resolution in palynological studies (Traverse, 2007). Poaceae (grass) pollen is a classic example of pollen morphological conservation, with > 12 000 species of grasses having a highly similar morphology that is consistent through the grass fossil pollen record, and that precludes further taxonomic subdivision in palynological studies (Mander *et al.*, 2013; Jardine *et al.*, 2019). It may be that the limited functional role of pollen grains (successful transfer of genetic material) means that continued morphological

experimentation within lineages is not selected for. In the case of the Asteraceae 2 clade, the evolution of a smaller, spiny pollen form (Fig. 2o) is thought to be advantageous for pollination relative to the larger, microechinate pollen of the Asteraceae 1 (Fig. 2i–l), because the stronger electrostatic attraction between the pollen grain and the receiving stigma increases the chances of successful pollen transfer from insect pollinator to flower (Inchaussandague *et al.*, 2018). Small and spiny pollen appears to have been highly successful ever since the Asteraceae 2 first diversified in the Oligocene and Miocene, and as such there may be limited scope for further refinement of this pollen type, with a concomitant lack of further exploration through morphospace.

Pollination ecology may play a more general role in controlling the arrangement of taxa in morphological space, via relationships with pollen size and ornamentation (Traverse, 2007; Mander *et al.*, 2020). Differences in pollination strategy, such as insect pollination in most Asterales vs bird, bat or wind pollination in some taxa (Oberprieler *et al.*, 2009; Vogel, 2015), may explain some aspects of morphospace occupation, although this requires further study with a focus on evolutionary trends within animal pollinators. Similarly, evolutionary developments in other plant organs such as flowers or capitula (the composite flower possessed by members of the Asteraceae) (Barreda *et al.*, 2010b; Roque & Funk, 2013) may have triggered pollen morphological evolution, and it would be interesting to investigate wider patterns of floral evolution in the Asterales. A promising approach for further research in this area would be analysis of floral morphospaces and disparity (Chartier *et al.*, 2014, 2017; Clark & Donoghue, 2018), to compare with the results presented here and to test for coordinated evolutionary changes through time.

This study has focused solely on extant taxa and as such likely provides an overly conservative estimate of changes in morphospace occupation through time. As noted earlier integrating fossil morphotypes in future analyses of pollen disparity would also help address whether the formation of distinct, clade-based groups in morphospace represents genuine rapid shifts in pollen morphology, or is due to the extinction of intermediate morphologies (Hopkins & Smith, 2015; Deline *et al.*, 2018). It may therefore resolve whether the evolution of pollen form has proceeded according to gradual or punctuated models of morphological evolution (Gould & Eldredge, 1977; Guillaume & Cooper, 2018; Sauquet & Magallon, 2018), and which of these should be preferred in future studies of pollen disparity. The fossil record of the Asterales is currently sparse before the Oligocene (Barreda *et al.*, 2010a), and to date, there have been limited attempts to directly integrate Asterales fossil pollen into a phylogenetic framework (although see Barreda *et al.*, 2015). Further work in this area may help to shed light on the drivers of Asterales pollen morphological evolution, especially during the explosive diversification and dispersal of the derived Asteraceae over the last *c.* 40 Ma (Mandel *et al.*, 2019; Palazzesi *et al.*, 2022).

We also acknowledge that the 113 taxa used in this study represent just a small fraction of the *c.* 27 000 extant species within the Asterales (Stevens, 2001). While the taxa were selected to be representative of the pollen morphologies and phylogenetic diversity within the Asterales, with the majority of families and tribes

included in the dataset, additional sampling would permit a more nuanced understanding of asteralean morphological evolution. This would aid in disentangling the relative influences of phylogenetic and functional diversity, as well as developmental processes and constraints, on Asterales pollen morphological disparity.

Finally, we echo calls for additional analyses of morphological disparity in plants, both as an important facet of biodiversity in its own right, and as a complementary metric to taxonomic, phylogenetic and functional diversity (Chartier *et al.*, 2014, 2017, 2021; Oyston *et al.*, 2016; Clark & Donoghue, 2018). Of particular interest is the distribution and partitioning of morphological disparity across spatial gradients and through time (Lupia, 1999; Wellman *et al.*, 2013; Mander, 2018; Chartier *et al.*, 2021), both focusing on individual organs or functional units (i.e. pollen grains and flowers) or combining these into whole plant analyses (e.g. Oyston *et al.*, 2016; Clark & Donoghue, 2018). Incorporating fossil data into such analyses, especially if supported by phylogenetic hypotheses, will enable a more nuanced understanding of disparity changes through the history of plant clades (Chartier *et al.*, 2017; Clark *et al.*, 2019; Schonenberger *et al.*, 2020). Such an approach will allow questions concerning the relationship between morphological disparity and taxonomic diversity (Foote, 1993, 1994; Lupia, 1999; Mander, 2018; Chartier *et al.*, 2021; Cole & Hopkins, 2021), morphological selectivity during extinction events (Foote, 1993; Lupia, 1999; Korn *et al.*, 2013; Cole & Hopkins, 2021) and integrated evolution across suites of morphological characters (Adams & Collyer, 2016; Chartier *et al.*, 2017), to be addressed, enhancing our understanding of the broad-scale patterns and processes of plant evolution.


Acknowledgements


PEJ acknowledges funding from the Deutsche Forschungsgemeinschaft (DFG, German Research Foundation) project number 443701866. LP, VDB and MCT acknowledge the Consejo Nacional de Investigaciones Científicas y Técnicas and Agencia Nacional de Investigaciones Científicas y Técnicas (PICT 2019–03011). We thank two anonymous reviewers for insightful comments on the manuscript. Open access funding enabled and organized by ProjektDEAL.


Author contributions

PEJ and LP designed the study. LP, MCT and VDB compiled the data and constructed the molecular phylogeny. PEJ analysed the data and led the writing of the paper, with input from LP, MCT and VDB. PEJ and LP contributed equally to this work.

ORCID

Viviana D. Barreda  <https://orcid.org/0000-0002-1560-1277>

Phillip E. Jardine  <https://orcid.org/0000-0002-8268-2353>

Luis Palazzesi  <https://orcid.org/0000-0001-8026-4679>

Data availability

All data and R code can be accessed at: <https://dx.doi.org/10.6084/m9.figshare.17104463>.

References

- Adams DC, Collyer ML. 2016. On the comparison of the strength of morphological integration across morphometric datasets. *Evolution* 70: 2623–2631.
- Ariizumi T, Toriyama K. 2011. Genetic regulation of sporopollenin synthesis and pollen exine development. *Annual Review of Plant Biology* 62: 437–460.
- Barker MS, Kane NC, Matvienko M, Kozik A, Michelmore RW, Knapp SJ, Rieseberg LH. 2008. Multiple paleopolyploidizations during the evolution of the compositae reveal parallel patterns of duplicate gene retention after millions of years. *Molecular Biology and Evolution* 25: 2445–2455.
- Barker MS, Li Z, Kidder TI, Reardon CR, Lai Z, Oliveira LO, Scascitelli M, Rieseberg LH. 2016. Most compositae (*Asteraceae*) are descendants of a paleohexaploid and all share a paleotetraploid ancestor with the *Calyceraceae*. *American Journal of Botany* 103: 1203–1211.
- Barreda VD, Palazzesi L, Telleria MC, Katinas L, Crisci JV. 2010a. Fossil pollen indicates an explosive radiation of basal Asteracean lineages and allied families during oligocene and miocene times in the Southern Hemisphere. *Review of Palaeobotany and Palynology* 160: 102–110.
- Barreda VD, Palazzesi L, Telleria MC, Katinas L, Crisci JV, Bremer K, Passalia MG, Corsolini R, Rodríguez Brizuela R, Bechis F. 2010b. Eocene patagonia fossils of the daisy family. *Science* 329: 1621.
- Barreda VD, Palazzesi L, Telleria MC, Olivero EB, Raine JI, Forest F. 2015. Early evolution of the angiosperm clade *Asteraceae* in the Cretaceous of Antarctica. *Proceedings of the National Academy of Sciences, USA* 112: 10989–10994.
- Benjamini Y, Hochberg Y. 1995. Controlling the false discovery rate: a practical and powerful approach to multiple testing. *Journal of the Royal Statistical Society, Series B* 57: 289–300.
- Blackmore S, Wortley AH, Skvarla JJ, Gabarayeva NI, Rowley JR. 2010. Developmental origins of structural diversity in pollen walls of compositae. *Plant Systematics and Evolution* 284: 17–32.
- Blackmore S, Wortley AH, Skvarla JJ, Robinson H. 2009. Evolution of pollen in the compositae. In: Funk VA, Susanna A, Stuessy TF, Bayer RJ, eds. *Systematics, evolution and biogeography of compositae*. Vienna, Austria: IAPT, 101–130.
- Blomberg SP, Garland TJ, Ives AR. 2003. Testing for phylogenetic signal in comparative data: behavioural traits are more labile. *Evolution* 57: 717–745.
- Bogotá-Ángel G, Huang H, Jardine PE, Chazot N, Salamanca S, Banks H, Pardo-Trujillo A, Plata A, Dueñas H, Star W *et al.* 2021. Climate and geological change as drivers of Mauritiinae palm biogeography. *Journal of Biogeography* 48: 1001–1022.
- Bryant D, Moulton V. 2004. Neighbor-net: an agglomerative method for the construction of phylogenetic networks. *Molecular Biology and Evolution* 21: 255–265.
- Cailliez F. 1983. The analytical solution of the additive constant problem. *Psychometrika* 48: 305–308.
- Chao A, Chiu CH, Jost L. 2010. Phylogenetic diversity measures based on hill numbers. *Philosophical Transactions of the Royal Society of London. Series B: Biological Sciences* 365: 3599–3609.
- Chao A, Chiu C-H, Jost L. 2014. Unifying species diversity, phylogenetic diversity, functional diversity, and related similarity and differentiation measures through hill numbers. *Annual Review of Ecology, Evolution, and Systematics* 45: 297–324.
- Chartier M, Jabbour F, Gerber S, Mitteroecker P, Sauquet H, von Balthazar M, Staedler Y, Crane PR, Schonenberger J. 2014. The floral morphospace – a modern comparative approach to study angiosperm evolution. *New Phytologist* 204: 841–853.
- Chartier M, Lofstrand S, von Balthazar M, Gerber S, Jabbour F, Sauquet H, Schonenberger J. 2017. How (much) do flowers vary? Unbalanced disparity among flower functional modules and a mosaic pattern of morphospace occupation in the order *Ericales*. *Proceedings of the Royal Society B: Biological Sciences* 284: 20170066.
- Chartier M, Von Balthazar M, Sontag S, Lofstrand S, Palme T, Jabbour F, Sauquet H, Schonenberger J. 2021. Global patterns and a latitudinal gradient of flower disparity: perspectives from the angiosperm order *Ericales*. *New Phytologist* 230: 821–831.
- Clark JW, Donoghue PCJ. 2018. Whole-genome duplication and plant macroevolution. *Trends in Plant Science* 23: 933–945.
- Clark JW, Puttick MN, Donoghue PCJ. 2019. Origin of horsetails and the role of whole-genome duplication in plant macroevolution. *Proceedings of the Royal Society B: Biological Sciences* 286: 20191662.
- Cole SR, Hopkins MJ. 2021. Selectivity and the effect of mass extinctions on disparity and functional ecology. *Science Advances* 7: eabf4072.
- Cooney CR, Bright JA, Capp EJR, Chira AM, Hughes EC, Moody CJA, Nouri LO, Varley ZK, Thomas GH. 2017. Mega-evolutionary dynamics of the adaptive radiation of birds. *Nature* 542: 344–347.
- Deline B, Greenwood JM, Clark JW, Puttick MN, Peterson KJ, Donoghue PCJ. 2018. Evolution of metazoan morphological disparity. *Proceedings of the National Academy of Sciences, USA* 115: E8909–E8918.
- Faith DP. 1992. Conservation evaluation and phylogenetic diversity. *Biological Conservation* 61: 1–10.
- Foote M. 1992. Rarefaction analysis of morphological and taxonomic diversity. *Paleobiology* 18: 1–16.
- Foote M. 1993. Discordance and concordance between morphological and taxonomic diversity. *Paleobiology* 19: 185–204.
- Foote M. 1994. Morphological disparity in Ordovician-Devonian crinoids and the early saturation of morphological space. *Paleobiology* 20: 320–344.
- Foote M. 1996a. Ecological controls on the evolutionary recovery of post-Paleozoic crinoids. *Science* 274: 1492–1495.
- Foote M. 1996b. Models of morphological diversification. In: Jablonski D, Erwin DH, Lipps JH, eds. *Evolutionary paleobiology*. Chicago, IL, USA: Chicago University Press, 62–86.
- Foote M. 1997. The evolution of morphological diversity. *Annual Review of Ecology and Systematics* 28: 129–152.
- Foote M. 1999. Morphological diversity in the evolutionary radiation of Paleozoic and post-Paleozoic crinoids. *Paleobiology* 25: 1–115.
- Fraser WT, Scott AC, Forbes AES, Glasspool IJ, Plotnick RE, Kenig F, Lomax BH. 2012. Evolutionary stasis of sporopollenin biochemistry revealed by unaltered Pennsylvanian spores. *New Phytologist* 196: 397–401.
- Friedman M. 2012. Parallel evolutionary trajectories underlie the origin of giant suspension-feeding whales and bony fishes. *Proceedings of the Royal Society B: Biological Sciences* 279: 944–951.
- Gould SJ, Eldredge N. 1977. Punctuated equilibria: the tempo and mode of evolution reconsidered. *Paleobiology* 3: 115–151.
- Guillermo T. 2018. DISPRITY: a modular R package for measuring disparity. *Methods in Ecology and Evolution* 9: 1755–1763.
- Guillermo T, Cooper N. 2018. Time for a rethink: time sub-sampling methods in disparity-through-time analyses. *Palaeontology* 61: 481–493.
- Hetherington AJ, Sherratt E, Ruta M, Wilkinson M, Deline B, Donoghue PCJ, Angielczyk K. 2015. Do cladistic and morphometric data capture common patterns of morphological disparity? *Palaeontology* 58: 393–399.
- Hopkins MJ. 2016. Magnitude versus direction of change and the contribution of macroevolutionary trends to morphological disparity. *Biological Journal of the Linnean Society* 118: 116–130.
- Hopkins MJ, Smith AB. 2015. Dynamic evolutionary change in post-Paleozoic echinoids and the importance of scale when interpreting changes in rates of evolution. *Proceedings of the National Academy of Sciences, USA* 112: 3758–3763.
- Hopkins MJ, St John K. 2018. A new family of dissimilarity metrics for discrete character matrices that include inapplicable characters and its importance for disparity studies. *Proceedings of the Royal Society B: Biological Sciences* 285: 20181784.
- Hughes M, Gerber S, Wills MA. 2013. Clades reach highest morphological disparity early in their evolution. *Proceedings of the National Academy of Sciences, USA* 110: 13875–13879.

- Hunt G. 2007. The relative importance of directional change, random walks, and stasis in the evolution of fossil lineages. *Proceedings of the National Academy of Sciences, USA* 104: 18404–18408.
- Huson DH, Bryant D. 2006. Application of phylogenetic networks in evolutionary studies. *Molecular Biology and Evolution* 23: 254–267.
- Inchaustandague M, Skigin D, Dolinko A, Tellería MC, Barreda VD, Palazzesi L. 2018. Spines, microspines and electric fields: a new look at the possible significance of sculpture in pollen of basal and derived *Asteraceae*. *Botanical Journal of the Linnean Society* 125: 794–801.
- Jaramillo CA, Rueda MJ, Mora G. 2006. Cenozoic plant diversity in the neotropics. *Science* 311: 1893–1896.
- Jardine PE, Gosling WD, Lomax BH, Julier ACM, Fraser WT. 2019. Chemotaxonomy of domesticated grasses: a pathway to understanding the origins of agriculture. *Journal of Micropalaeontology* 38: 83–95.
- Jardine PE, Palazzesi L, Tellería MC, Barreda VD. 2022. Data and code for ‘Why does pollen morphology vary? Evolutionary dynamics and morphospace occupation in the largest angiosperm order (Asterales)’. *Figshare*, doi: 10.6084/m9.figshare.17104463.
- Jiménez F, Katinas L, Tellería MC, Crisci JV. 2004. *Salcedoa* gen. nov., a biogeographic enigma in the Caribbean Mutisieae (*Asteraceae*). *Systematic Botany* 29: 987–1002.
- Kaderit JW, Jeffrey C, eds. 2007. Flowering plants. Eudicots: asterales. *The families and genera of vascular plants*. Berlin Heidelberg, Germany: Springer-Verlag.
- Katinas L, Crisci JV, Tellería MC, Barreda V, Palazzesi L. 2010. Early history of *Asteraceae* in Patagonia: evidence from fossil pollen grains. *New Zealand Journal of Botany* 45: 605–610.
- Kembel SW, Cowan PD, Helmus MR, Cornwell WK, Morlon H, Ackerly DD, Blomberg SP, Webb CO. 2010. PICANTE: R tools for integrating phylogenies and ecology. *Bioinformatics* 26: 1463–1464.
- Knight CA, Clancy RB, Götzenberger L, Dann L, Beaulieu JM. 2010. On the relationship between pollen size and genome size. *Journal of Botany* 2010: 1–7. Article ID 612017.
- Korn D, Hopkins MJ, Walton SA. 2013. Extinction space – a method for the quantification and classification of changes in morphospace across extinction boundaries. *Evolution* 67: 2795–2810.
- Kriebel R, Khabbazian M, Sytsma KJ. 2017. A continuous morphological approach to study the evolution of pollen in a phylogenetic context: an example with the order *Myrtales*. *PLoS ONE* 12: e0187228.
- Landis JB, Soltis DE, Li Z, Marx HE, Barker MS, Tank DC, Soltis PS. 2018. Impact of whole-genome duplication events on diversification rates in angiosperms. *American Journal of Botany* 105: 348–363.
- Lloyd GT. 2016. Estimating morphological diversity and tempo with discrete character-taxon matrices: implementation, challenges, progress, and future directions. *Biological Journal of the Linnean Society* 118: 131–151.
- Lloyd GT. 2018. Journeys through discrete-character morphospace: synthesizing phylogeny, tempo, and disparity. *Palaeontology* 61: 637–645.
- Lloyd GT, Wang SC, Brusatte SL. 2012. Identifying heterogeneity in rates of morphological evolution: discrete character change in the evolution of lungfish (*Sarcopterygii*, Dipnoi). *Evolution* 66: 330–348.
- Lupia R. 1999. Discordant morphological disparity and taxonomic diversity during the Cretaceous angiosperm radiation: north American pollen record. *Paleobiology* 25: 1–28.
- Mackenzie G, Boa AN, Diego-Taboada A, Atkin SL, Sathyapalan T. 2015. Sporopollenin, the least known yet toughest natural biopolymer. *Frontiers in Materials* 2: 1–5.
- Mandel JR, Dikow RB, Siniscalchi CM, Thapa R, Watson LE, Funk VA. 2019. A fully resolved backbone phylogeny reveals numerous dispersals and explosive diversifications throughout the history of *Asteraceae*. *Proceedings of the National Academy of Sciences, USA* 116: 14083–14088.
- Mander L. 2016. A combinatorial approach to angiosperm pollen morphology. *Proceedings of the Royal Society of London B: Biological Sciences* 283: 20162033.
- Mander L. 2018. The latitudinal distribution of morphological diversity among holocene angiosperm pollen grains from eastern north America and the neotropics. *Integrative and Comparative Biology* 58: 1170–1178.
- Mander L, Li M, Mio W, Fowlkes CC, Punyasena SW. 2013. Classification of grass pollen through the quantitative analysis of surface ornamentation and texture. *Proceedings of the Royal Society of London B: Biological Sciences* 280: 20131905.
- Mander L, Parins-Fukuchi C, Dick CW, Punyasena SW, Jaramillo C. 2020. Phylogenetic and ecological correlates of pollen morphological diversity in a neotropical rainforest. *Biotropica* 53: 74–85.
- Matamoro-Vidal A, Prieu C, Furness CA, Albert B, Gouyon PH. 2016. Evolutionary stasis in pollen morphogenesis due to natural selection. *New Phytologist* 209: 376–394.
- McDonald-Spicer C, Knerr NJ, Encinas-Viso F, Schmidt-Lebuhn AN. 2019. Big data for a large clade: bioregionalization and ancestral range estimation in the daisy family (*Asteraceae*). *Journal of Biogeography* 46: 255–267.
- Nadot S, Furness CA, Sannier J, Penet L, Triki-Teurtroy S, Albert B, Ressayre A. 2008. Phylogenetic comparative analysis of microsporogenesis in angiosperms with a focus on monocots. *American Journal of Botany* 95: 1426–1436.
- Neuwirth E. 2014. *R.COLORBREWER: ColorBrewer palettes*. R package v.1.1-2. [WWW document] URL <https://CRAN.R-project.org/package=RColorBrewer>.
- Oberprieler C, Himmelreich S, Källersjö M, Vallés J, Watson LE, Vogt R. 2009. Anthemideae. In: Funk VA, Susanna A, Steussy TF, Bayer RJ, eds. *Systematics, evolution, and biogeography of Compositae*. Vienna, Austria: International Association for Plant Taxonomy (IAPT), 631–666.
- Oksanen J, Blanchet FG, Friendly M, Kindt R, Legendre P, McGlenn D, Minchin PR, O’Hara RB, Simpson GL, Solymos P *et al.* 2020. *VEGAN: community ecology package*. R package v.2.5-7 [WWW document] URL <https://CRAN.R-project.org/package=vegan>.
- Oyston JW, Hughes M, Wagner PJ, Gerber S, Wills MA. 2015. What limits the morphological disparity of clades? *Interface Focus* 5: 20150042.
- Oyston JW, Hughes M, Gerber S, Wills MA. 2016. Why should we investigate the morphological disparity of plant clades? *Annals of Botany* 117: 859–879.
- Palazzesi L, Hidalgo O, Barreda VD, Forest F, Höhna S. 2022. The rise of grasslands is linked to atmospheric CO₂ decline in the late Palaeogene. *Nature Communications* 13: 293.
- Panero JL, Crozier BS. 2016. Macroevolutionary dynamics in the early diversification of *Asteraceae*. *Molecular Phylogenetics and Evolution* 99: 116–132.
- Paradis E, Schliep K. 2019. APE 5.0: an environment for modern phylogenetics and evolutionary analyses in R. *Bioinformatics* 35: 526–528.
- R Core Team. 2021. *R: a language and environment for statistical computing*. v.4.0.4 [WWW document] URL <http://www.R-project.org>.
- R Studio Team 2021. *RSTUDIO: integrated development environment for R*. v.1.4.1717 [WWW document] URL <https://www.rstudio.com>.
- Revell LJ. 2012. PHYTOOLS: an R package for phylogenetic comparative biology (and other things). *Methods in Ecology and Evolution* 3: 217–223.
- Roque N, Funk VA. 2013. Morphological characters add support for some members of the basal grade of *Asteraceae*. *Botanical Journal of the Linnean Society* 171: 568–586.
- Roy K, Foote M. 1997. Morphological approaches to measuring biodiversity. *Trends in Ecology & Evolution* 12: 277–281.
- Sakamoto M, Ruta M. 2012. Convergence and divergence in the evolution of cat skulls: temporal and spatial patterns of morphological diversity. *PLoS ONE* 7: e39752.
- Sauquet H, Magallon S. 2018. Key questions and challenges in angiosperm macroevolution. *New Phytologist* 219: 1170–1187.
- Schliep K. 2011. PHANGORN: phylogenetic analysis in R. *Bioinformatics* 27: 592–593.
- Schonenberger J, von Balthazar M, Lopez Martinez A, Albert B, Prieu C, Magallon S, Sauquet H. 2020. Phylogenetic analysis of fossil flowers using an angiosperm-wide data set: proof-of-concept and challenges ahead. *American Journal of Botany* 107: 1433–1448.
- Sidlauskas B. 2008. Continuous and arrested morphological diversification in sister clades of characiform fishes: a phylomorphospace approach. *Evolution* 62: 3135–3156.
- Soetaert K. 2019. *PLOT3D: plotting multi-dimensional data*. R package v.1.3 [WWW document] URL <https://CRAN.R-project.org/package=plot3D>.
- Soltis DE, Albert VA, Leebens-Mack J, Bell CD, Paterson AH, Zheng C, Sankoff D, Depamphilis CW, Wall PK, Soltis PS. 2009. Polyploidy and angiosperm diversification. *American Journal of Botany* 96: 336–348.
- Soltis PS, Soltis DE. 2016. Ancient WGD events as drivers of key innovations in angiosperms. *Current Opinion in Plant Biology* 30: 159–165.

- Stevens PF. 2001. *Angiosperm phylogeny website*. v.14, July 2017 [and more or less continuously updated since]. [WWW document] URL <http://www.mobot.org/MOBOT/research/APweb/> [accessed 20 January 2022].
- Tellería MC. 2008. Taxonomic significance of pollen types in the Guyana Highland-centred genera (Asteraceae, Mutisioideae). *Botanical Journal of the Linnean Society* 156: 327–340.
- Tellería MC. 2017. Spines vs. microspines: an overview of the sculpture exine in selected basal and derived Asteraceae with focus on Asteroideae. *Journal of Plant Research* 130: 1023–1033.
- Tellería MC, Barreda V, Palazzesi L, Katinas L. 2010. Echinatoid fossil pollen of Asteraceae from the late oligocene of Patagonia: an assessment of its botanical affinity. *Plant Systematics and Evolution* 285: 75–81.
- Tellería MC, Katinas L. 2004. A palynologic and comparative study of *Chaetanthera* (Asteraceae, Mutisieae) and allied genera. *Systematic Botany* 29: 752–773.
- Tellería MC, Katinas L. 2009. New insights into the pollen morphology of *Mutisia* (Asteraceae, Mutisieae). *Plant Systematics and Evolution* 280: 229–241.
- Tellería MC, Sancho G, Funk VA, Ventosa I, Roque N. 2013. Pollen morphology and its taxonomic significance in the tribe Gochnatieae (Compositae, Gochnatioideae). *Plant Systematics and Evolution* 299: 935–948.
- Traverse A. 2007. *Paleopalynology*. Dordrecht, the Netherlands: Springer.
- Vogel S. 2015. Vertebrate pollination in Compositae: floral syndromes and field observations. *Stapfia* 103: 5–26.
- Warton DI, Wright ST, Wang Y. 2012. Distance-based multivariate analyses confound location and dispersion effects. *Methods in Ecology and Evolution* 3: 89–101.
- Wellman CH, Steemans P, Vecoli M. 2013. Palaeophytogeography of Ordovician–Silurian land plants. In: Harper DAT, Servais T, eds. *Early palaeozoic biogeography and palaeogeography*. London, UK: Geological Society, 461–476.
- Wickham H, François R, Henry L, Müller K. 2021. *DPLYR: a grammar of data manipulation*. R package v.1.0.7 [WWW document] URL <https://CRAN.R-project.org/package=dplyr>.
- Wills MA, Briggs DEG, Fortey RA. 1994. Disparity as an evolutionary index: a comparison of Cambrian and recent arthropods. *Paleobiology* 20: 93–130.
- Wortley AH, Blackmore S, Chissole WF, Skvarla JJ. 2012. Recent advances in Compositae (Asteraceae) palynology, with emphasis on previously unstudied and unplaced taxa. *Grana* 51: 158–179.
- Wortley AH, Funk VA, Robinson H, Skvarla JJ, Blackmore S. 2007. A search for pollen morphological synapomorphies to classify rogue genera in Compositae (Asteraceae). *Review of Palaeobotany and Palynology* 146: 169–181.
- Wortley AH, Funk VA, Skvarla JJ. 2008. Pollen and the evolution of Arctotideae (Compositae). *The Botanical Review* 74: 438–466.
- Woutersen A, Jardine PE, Bogotá-Angel G, Zhang H-X, Silvestro D, Antonelli A, Gogna E, Erkens RHJ, Gosling WD, Dupont-Nivet G *et al.* 2018. A novel approach to study the morphology and chemistry of pollen in a phylogenetic context, applied to the steppe-desert taxon *Nitraria* L. (Nitrariaceae). *PeerJ* 6: e5055.
- Yu G. 2020. *SCATTERPIE: scatter pie plot*. R package v. 0.1.7 [WWW document] URL <https://CRAN.R-project.org/package=scatterpie>.
- Yu G, Smith D, Zhu H, Guan Y, Lam TT-Y. 2017. GGTREE: an R package for visualization and annotation of phylogenetic trees with their covariates and other associated data. *Methods in Ecology and Evolution* 8: 28–36.
- Zaffos AA. 2019. *VELOCIRAPTR: fossil analysis*. R package v. 1.1.0 [WWW document] URL <https://CRAN.R-project.org/package=velociraptr>.

Supporting Information

Additional Supporting Information may be found online in the Supporting Information section at the end of the article.

Fig. S1 Phylogenetic signal, measured as Blomberg's K , on each axis of the principal coordinates analysis (PCO) morphospace.

Fig. S2 Alternative phylomorphospace ordinations.

Fig. S3 Cluster analysis of the maximum observable rescaled distance (MORD) matrix of the coded character data.

Fig. S4 Neighbor-Net of the maximum observable rescaled distance (MORD) matrix of the coded character data.

Fig. S5 States for key characters on axes 1 and 2 of the principal coordinates analysis (PCO) morphospace.

Fig. S6 Within-clade disparity, showing complementary plots to Fig. 4(a) in the main paper.

Fig. S7 Disparity through time plots.

Fig. S8 Biogeographic occurrence of taxa in this study.

Fig. S9. Morphological disparity and phylogenetic diversity of Asteraceae subfamilies.

Table S1 Pollen characters and states.

Please note: Wiley Blackwell are not responsible for the content or functionality of any Supporting Information supplied by the authors. Any queries (other than missing material) should be directed to the *New Phytologist* Central Office.